Annals of Mathematical Sciences and Applications
Volume 4, Number 2, 367–393, 2019

Space-time analysis and beyond: toward a better understanding of Camassa-Holm equation

Chueh-Hsin Chang, Ching-Hao Yu, and Tony Wen-Hann Sheu*

Camassa-Holm (CH) equation for modeling shallow water wave will be analyzed through direct scattering analysis. Thanks to this analysis in spectral domain, some physically meaningful wave propagation features that can by no means be obtained from the analysis in the space-time domain are exhibited. To broaden our understanding of the CH equation, in this article the study underlying the scattering analysis is performed in spectral domain and the solution of CH equation is computed by the finite difference method in time domain. We aim to get some missing details in the space-time analysis. The detailed wave transmission and reflection in the CH equation, subject to the chosen initial condition, shall be theoretically enlightened.

AMS 2000 subject classifications: Primary 78A46, 81U40; secondary 37K10.

1. Introduction

Shallow water wave can be modeled by different partial differential equations [1, 2, 3, 4, 5] since the development of Korteweg–de Vries (KdV) equation in 1895. In this paper, the Camassa-Holm (CH) equation [1, 2] is considered. This nonlinear equation is dispersive in nature for a function u of two variables, which are x (space variable) and t (time variable). CH equation shown below has been regarded as an important member of the completely integrable equations.

$$u_t - u_{xxt} + 2\kappa u_x + 3uu_x = 2u_x u_{xx} + uu_{xxx}. \tag{1}$$

In CH equation, the integrability, bi-Hamiltonian structure, infinite number of conservation laws [1], Lax pair and its inverse scattering processes [6] have been well-studied. CH equation possesses many mathematical properties undiscovered in KdV equation. Moreover, this equation is the first

*Corresponding author.

equation capable of exhibiting the phenomena of soliton interaction and wave breaking. The CH equation has therefore been considered as a master equation for modeling shallow water wave (see [7] for the references therein).

There have been many numerical methods proposed to solve the CH equation in space-time domain [8, 9, 10]. However, wave propagation details in spectral domain cannot be observed. In order to get a thorough understanding of the wave propagation features in shallow water equation, one can take the integrability in CH equation into account in spectral domain. Transformation of equations from one to the other is an important technique to solve nonlinear and dispersive differential equations. The differential equation defined in the space-time domain needs to be transformed to its equivalent equations defined in a domain with two new variables. Through the use of these new variables the differential equation is transformed to a much simple differential equation or even an algebraic equation. The most well-known transformations in the context of differential equations are the Laplace and Fourier transforms. In the discussion of the integrability of CH equation, the transformation method normally employed is the inverse scattering transform (IST) [6].

IST is now well accepted as one of the most important developments in the community of mathematical physics in the last of the century. The key theme in IST is to recover the potential from its time evolving scattering data in spectral domain. The technique of inverse scattering involves analyzing the isospectral problem from the corresponding Lax pair. In the isospectral problem, an incident wave in the form of the eigenfunction emerging from one side of the domain can be divided into a part transmitted to the other side and a reflected part accounting for the eigenfunction, respectively. The sum of the transmission and reflection waves equals the original incident wave [6]. The data include the eigenvalues, and the reflected wave content called the scattering data. The degree of wave reflection is essential in the study of integrable equations. This can be seen from the following two examples. In [11], the multi-soliton solutions have been constructed for the case without reflected wave. However, it is physically reasonable that an incident wave can completely transmit if there is no wave being reflected. Therefore, there exists just a solitary wave emerging along the real line without exhibiting its oscillatory tails [12]. In contrast to this example, Boutet de Monvel et al. [13] observed the long-time asymptotic nature in the classical solutions. They found that as the time becomes large enough, not only the multi-soliton will be seen but also its oscillatory tail shall appear owing to the reflection waves contributing to the propagation of incident wave. Because of these important mathematical studies, now we know quite well about the

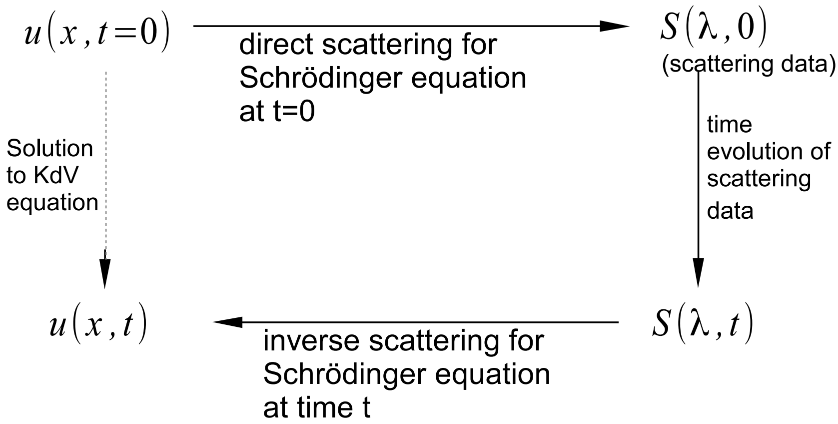

Figure 1: The diagram linking the direct and inverse scatterings for the KdV equation.

CH equation. However, there are still some questions awaiting for further investigation, such as the difference between the computed CH solutions in space-time and spectral domains (the solutions found by inverse scattering transform); the dynamics of reflection wave, and how a reflection wave can affect the dynamics of CH equations.

In this paper, the CH solution will be computed by the FDTD (finite difference in time domain method) and in spectral analysis we will perform direct scattering analysis on the CH equation as well [14]. The explicit expression of the ratio of the reflection/transmission coefficients which measure the ratio of reflected/transmitted waves will be presented. This is a new attempt to the best of authors' knowledge. We also aim to reveal more clearly the relation between the solution of CH equation and the corresponding reflection coefficient.

In Section 4 some theoretical backgrounds closely related to the development of finite difference numerical scheme will be briefly summarized. The solutions found in space-time and spectral domains will be introduced in Sections 4.3, 4.4 and in Section 5, respectively. Discussion of the transmission and reflection coefficients will be given in Section 6. Some remarks and conclusions are drawn in Section 7.

2. The method of scattering transform

IST can be regarded as a nonlinear version of the Fourier transform. The method of IST was first applied to KdV equation $u_t - 6uu_x + uu_{xxx} = 0$ [15].

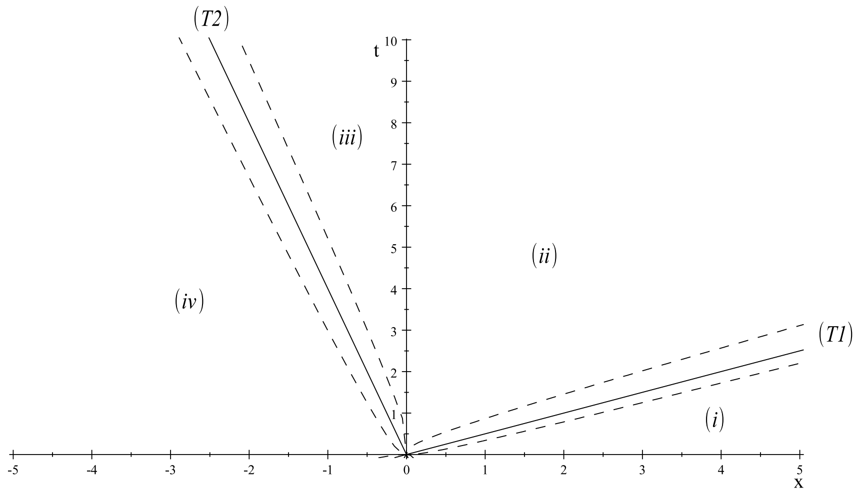

Figure 2: The numerically predicted long-time asymptotics of the CH solutions using the numerical method presented in Section 4 in six distinct regions.

This equation is integrable and is associated with a linear ordinary differential equation (LODE), which is the Schrödinger equation $-\frac{d^2\psi}{dx^2}+u\,(x,t)\,\psi = k^2\psi$ containing the spectral parameter $\lambda = k^2$. Note that the spectral parameter does not change with time [15]. While x and t are considered as independent variables in KdV equation, in the linear Schrödinger equation, x is an independent variable and λ and t are regarded as two parameters. It is quite normal that the potential $u(x,t)$ vanishes at each fixed t as x becomes infinite. As a result, a scattering scenario can be created for the related LODE (or Schrödinger equation), in which the potential $u(x,t)$ can be uniquely related to some scattering data $S(\lambda,t)$. The scattering data having association with the LODE (Schrödinger equation) consist of a reflection coefficient which is a function of the spectral parameter λ, a finite set of constants λ_j corresponding to a set of poles of the transmission coefficient in the upper half of the complex plane, and the bounded-state norming constants. The number for each bounded-state pole λ_j is equal to the number of poles. The potential $u(x,t)$ in the LODE can be uniquely determined by the corresponding scattering data and vice versa. Take the integrable KdV equation as an example, the IST method can be explained by the diagram schematically shown in Fig. 1:

The IST method involves the so-called direct scattering problem, which is defined as the problem of determining $S(\lambda,t)$ for all λ values from $u(x,t)$

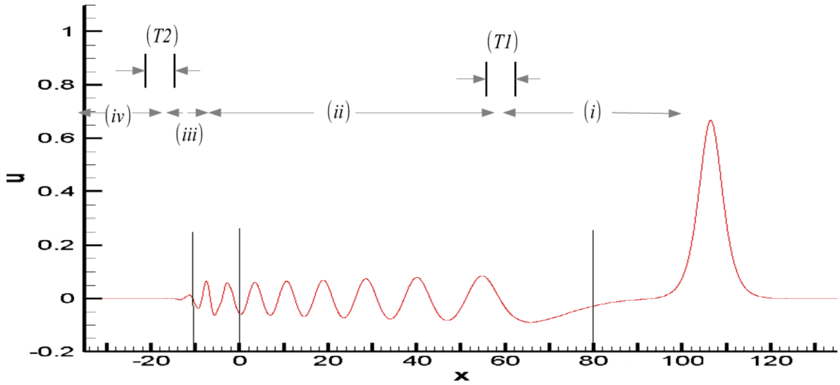

Figure 3: The computed solution of u at $t = 40$, $q_0 = \frac{1}{2}$ based on the finite difference method presented in Section 4.

given for all x values, for the Schröinger equation and the inverse scattering problem for Schröinger equation, which is defined as the problem of determining $u(x,t)$ from $S(\lambda, t)$. It is amazing that as $t \to 0$ the limiting value of $u(x,t)$ agrees with the initial profile $u(x,0)$.

The IST method for solving the KdV equation was firstly proposed by Gardner et al. in 1967 [15]. By the Gel'fand-Dorfmann theory [1], it is known that the nonlinear KdV equation is in fact a compatibility condition for the two linear equations, namely, the isospectral eigenvalue problem $-\frac{d^2\psi}{dx^2} + u\,(x,t)\,\psi = k^2\psi$, and the linear evolution equation $\psi_t = (2u+4\lambda)\psi_x - u_x\psi$ for the eigenfunction ψ. In short, the solution of KdV equation is sought subject to the compatibility of two linear equations i.e., $\psi_{xxt} = \psi_{txx}$, and isospectrality ($\frac{d\lambda}{dt} = 0$). Consequently, one can apply the method of IST to solve the solution of KdV equation. This method was later extended to solve the nonlinear Schrödinger equation, the sine-Gordon equation [16], the Toda lattice equation [17], the Kadomtsev–Petviashvili (KP) equation [18], and so on.

3. Scattering analysis of CH equation

The solution of CH equation (1) shall be sought subject to the specified initial condition given by

$$u\,(x,0) = \begin{cases} \frac{A(A+1+\log(e^x - A))}{e^x}, & \text{for } x \geq \log\,(1+A)\,, \\ \frac{A\left(A+1+\log\left((1+A)^2 e^{-x} - A\right)\right)}{(1+A)^2 e^{-x}}, & \text{for } x < \log\,(1+A)\,. \end{cases} \tag{2}$$

In the above, $q_0 \in (0,1)$ is a given constant and $A = \frac{q_0}{1-q_0}$. The reason of choosing (2) as the initial data in the current study is as follows. Under the above initial condition, the resulting scattering data have non-zero reflection coefficients [19]. Provided that the reflection coefficient is zero, the process of performing IST becomes comparatively easy. Moreover, for the case with a single soliton the corresponding asymptotic exists. This prescribed initial condition can be transformed to the Schrödinger type operator with the corresponding delta-function potential. Subject to this initial condition, both the soliton and the oscillatory phenomena can be exhibited in the long-time asymptotics. Moreover, by applying the finite difference method in [20] one can obtain the asymptotic CH solution from the known scattering data under the initial condition given in (2).

Given the initial condition, the method underlying IST involves the solution step known as the forward scattering. In this step detailed in Section 3.1, we aim to find the Lax pair, which comprises two linear operators. The next step, detailed in Section 3.2, is to get the evolution of eigenfunctions associated with their corresponding eigenvalues, norming constants, and the reflection coefficients. The final step schematic in Fig. 1 involves performing inverse scattering procedure, which will not be dealt with in this study. As opposed to the direct scattering problem of finding the scattering matrix (or data) from the given potential, by solving the linear Gel'fand-Levitan-Marchenko integral equation to get the solution in (x,t).

3.1. Direct scattering

The step of conducting inverse scattering transform is to perform firstly the forward scattering analysis. This direct scattering process involves finding the Lax pair of the CH equation, which is composed of

$$\frac{1}{w}\left(-\psi_{xx} + \frac{1}{4}\psi\right) = \lambda\psi, \tag{3}$$

$$\psi_t = -\left(\frac{1}{2\lambda} + u\right)\psi_x + \frac{1}{2}u_x\psi. \tag{4}$$

In (3), $w = u - u_{xx} + 1$ denotes the momentum. The solution to the CH equation is sought subject to the initial condition which satisfies the following conditions for some integer $l \geq 1$.

$$w\,(x,0) > 0, \quad \forall x \in \mathbb{R}, \tag{5}$$

(6)
$$w(x,0) \in \left\{ v \in H^3(\mathbb{R}) \middle| \int_{\mathbb{R}} (1+|x|)^{1+l} \left(|v(x)-\kappa| + |v'(x)| + |v''(x)| \right) dx \right\}$$

It was shown in [6] that $w(x,t) > 0$ for $t > 0$ provided that the initial condition (5) holds. By the Liouville transformation [21]

$$\tilde{\psi}(y) = (w(x,t))^{\frac{1}{4}} \psi(x), \tag{7}$$

$$y = x - \int_x^{\infty} \left(\sqrt{w(r,t)} - 1 \right) dr, \tag{8}$$

equation (3) can be reformulated as a spectral problem containing the operator of the Schrödinger type

$$L\tilde{\psi} := -\tilde{\psi}_{yy} + q(y,t)\tilde{\psi} = k^2 \tilde{\psi}, \tag{9}$$

where $\tilde{\psi} = \tilde{\psi}(y,k,t)$. It is noted that k and λ relate themselves by

$$\lambda = \frac{1}{4} + k^2. \tag{10}$$

Moreover, one can get

$$q(y,t) = \frac{w_{yy}(y,t)}{4w(y,t)} - \frac{3}{16}\frac{(w_y)^2(y,t)}{w^2(y,t)} + \frac{1-w(y,t)}{4w(y,t)} \tag{11}$$

with $w(y,t) = w(x(y),t)$. From (6) we have

$$\int_{\mathbb{R}} (1+|y|)^2 q(y,0)\, dy < \infty.$$

Thanks to the previous work in [22], $\mu_1, \cdots, \mu_N \in \mathbb{R}$ exist for some $N \in \mathbb{N}$ and, in turn, the spectra at a finite number of discrete $k = i\mu_1, \cdots, i\mu_N$ exist. All the eigenvalues are simple with the eigenfunction $\tilde{\psi}_j(y) = \tilde{\psi}(y, i\mu_j, 0)$ for $k = i\mu_j$. Let γ_j be a constant satisfying the following assumption

$$\tilde{\psi}_j(y) = \gamma_j e^{-\mu_j y} + o(1) \text{ as } y \to \infty.$$

In the continuous spectrum context, the eigenfunction $\hat{\psi} = \hat{\psi}(y,k)$ for $k \in \mathbb{R}$ satisfies

$$\hat{\psi} \sim \begin{cases} e^{-iky} + \tilde{R}(k)\, e^{iky}; \text{ as } y \to \infty, \\ \tilde{T}(k)\, e^{-iky}; \text{ as } y \to -\infty. \end{cases} \tag{12}$$

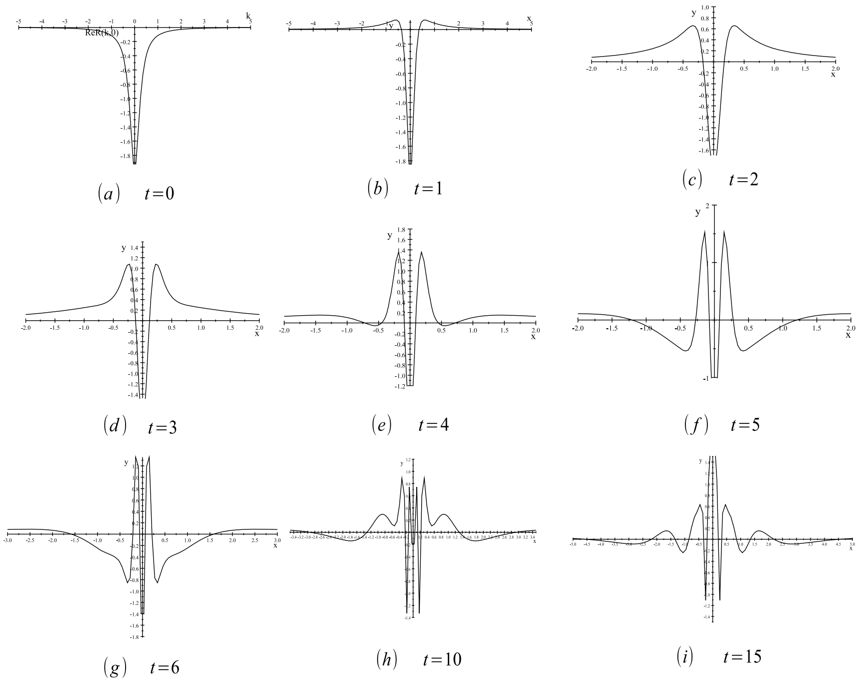

Figure 4: The time dependence of $\Re\big(R(k,t)\big)$ from $t=0$ to $t=15$ at $q_0=\frac{1}{2}$.

In the above equation, $\tilde{T}\,(k)$ and $\tilde{R}\,(k)$ are called as the transmission and reflection coefficients, respectively. The eigenvalue μ_j, the constants γ_j, and the reflection coefficient $\tilde{R}\,(k)$ constitute the so-called scattering data defined as $\left\{\tilde{R}\,(k)\,,\mu_j,\gamma_j\right\}$ $(j=1,...,N)$. Let $T\,(k)$ and $R\,(k)$ be the transmission and reflection coefficients of the spectral problem (3). The four transmission and reflection functions $T\,(k)\,,R\,(k)$ and $\tilde{T}\,(k)\,,\tilde{R}\,(k)$ are related themselves with the two equations given below

$$T\,(k)=\tilde{T}\,(k)\,e^{ikH_{-1}(w)},\;\; R\,(k)=\tilde{R}\,(k)\,, \tag{13}$$

where $H_{-1}\,(w)\equiv\int_{\mathbb{R}}\left(\sqrt{w\,(r,t)}-1\right)dr$. It is noted that $H_{-1}\,(w)$ is one of the conservation laws [23].

3.2. Evolution of scattering data

From (4), which describes the time evolution of the eigenfunction in (3), together with the asymptotic expressions in (12), we can get the isospectral

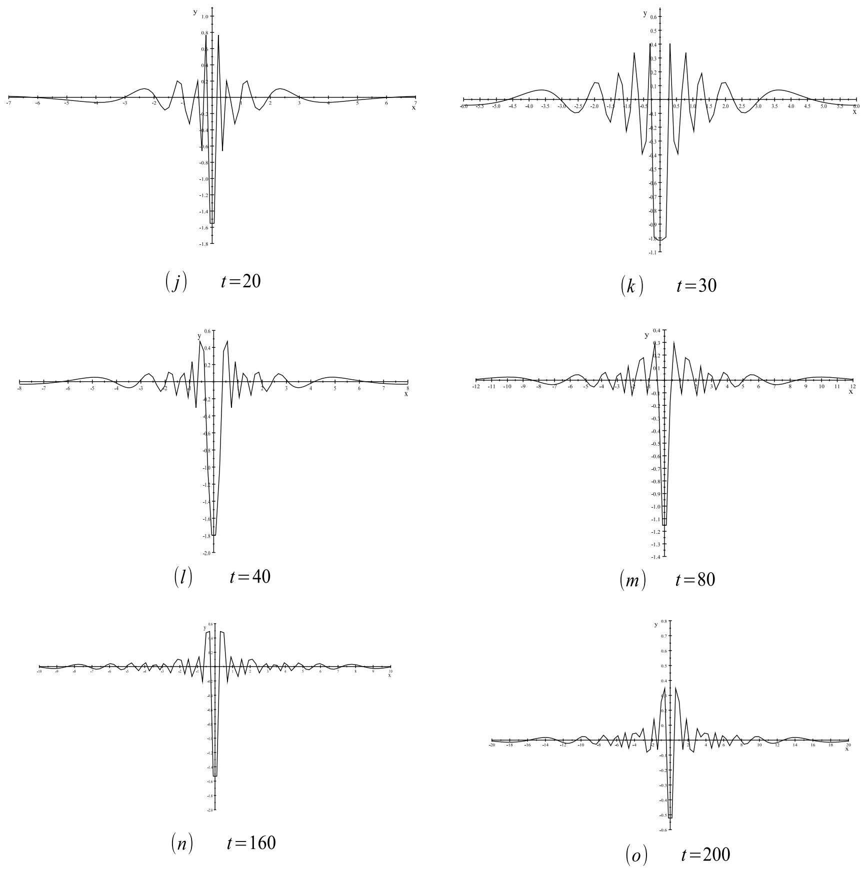

Figure 5: The time dependence of $\Re\big(R(k,t)\big)$ from $t=20$ to $t=200$ at $q_0=\frac{1}{2}$.

property

$$\mu_i\,(t)=\mu_i,\; i=1,...,N.$$

The dependence of $R(k)$ and γ_j on time can be derived as [21]

$$R(k,t)=R(k)e^{-ikt/(1/4+k^2)},\;\gamma_j\,(t)=\gamma_j e^{\mu_j t/2(1/4-\mu_j^2)},\;\text{for } t>0. \tag{14}$$

3.3. Inverse scattering

The inverse scattering transform is mathematically equivalent to the process of recovering the solution u from the scattering data derived in the forward scattering step. For example, the solution of KdV equation corresponds to the potential of Schrödinger type. The KdV solution can be therefore obtained by solving the so-called Gel'fand- Levitan-Marchenko (GLM) integral equation for the KdV equation [15]

$$K(y,r,t)+f(y+r,t)+\int_y^\infty K(y,z,t)\,f(r+z,t)\,dz=0,\quad r>y, \tag{15}$$

where

$$f(z,t)=\sum_{j=1}^{N}\gamma_j^2(t)\,e^{-\mu_j z}+\frac{1}{2\pi}\int_{-\infty}^{\infty}R(k,t)\,e^{ikz}dk. \tag{16}$$

The operator for the spectral problem of CH equation is much different from that of the KdV equation. We need, as a result, to recover the solution of CH equation after deriving the potential q in (9) from the GLM equation

$$q(y,t)=-2\frac{d}{dy}K(y,y,t). \tag{17}$$

Some results concerning the IST performed on the CH equation are now available in the literature, for example, [6, 14, 24, 25]. In [6], Constantin stated that $w(y,t)$ is equal to $C^4(y,t)$, which satisfies

$$C_{yy}=C\left(q(y,t)+\frac{1}{4}\right)-\frac{1}{4C^3},\ \lim_{|y|\to\infty}C(y,t)=1.$$

In order to eliminate the difficulties in solving the nonlinear differential equation stated above, another version of IST was proposed in [14] as follows. Consider $\psi(y,t)$ as the unique solution to the equation

$$\phi_{yy}=\left(q(y,t)+\frac{1}{4}\right)\phi \tag{18}$$

subject to the asymptotic behavior given by

$$\psi(y,t)\approx e^{-\frac{y}{2}}\ \text{and}\ f_y(y,t)\approx\frac{-1}{2}e^{-\frac{y}{2}}\ \text{as}\ y\to\infty. \tag{19}$$

If $H_t:\mathbb{R}\to\mathbb{R}$ is the bijection given by

$$H_t(y)=\int_{-\infty}^{y}\frac{1}{\psi^2(\xi,t)}d\xi$$

then we can get $H_t(y) = e^x$ and

$$w(x,t) = e^{2x}\psi^4\left(H_t^{-1}(e^x), t\right).$$

The momentum w can now be expressed in the following parametric form with the variable y being considered as a parameter.

$$\left\{\begin{array}{ll} w(y,t) & = e^{2\ln H_t(y)}\psi^4(y,t), \\ & = H_t^2(y)\,\psi^4(y,t), \\ & \\ x(y,t) & = \ln H_t(y) = \ln \int_{-\infty}^{y} \frac{1}{\psi^2(\xi,t)} d\xi. \end{array}\right. \tag{20}$$

Note that one can verify the inverse processes either by the example given in [14] or by the initial condition (2). In the later case, at $t = 0$ the unique solution $r(y,0)$ to $\phi_{yy} = \left(q(y,0) + \frac{1}{4}\right)\phi$ can be found explicitly as

$$\psi(y,0) = \left\{\begin{array}{ll} e^{\frac{-y}{2}}, & y \geq 0, \\ q_0 e^{\frac{y}{2}} + (1-q_0)\, e^{\frac{-y}{2}}, & y < 0. \end{array}\right.$$

Given the above expression of $\psi(y,0)$, we can get

$$H_0(y) = \left\{\begin{array}{ll} \frac{1}{1-q_0}\frac{1}{q_0+(1-q_0)e^{-y}}, & y \leq 0, \\ \frac{1}{1-q_0} + e^y - 1, & y > 0. \end{array}\right.$$

and then the solution

$$\psi\left(H_0^{-1}(e^x), 0\right) = \left\{\begin{array}{ll} (e^x - A)^{\frac{-1}{2}}, & x \geq \ln(1+A), \\ q_0\left((1+A)^2 e^{-x} - A\right)^{\frac{-1}{2}} + & \\ (1-q_0)\left((1+A)^2 e^{-x} - A\right)^{\frac{1}{2}}, & x < \ln(1+A). \end{array}\right.$$

Finally, one can easy verify that $e^{2x}\psi^4\left(H_0^{-1}(e^x), 0\right)$ equals $w(x,0)$ in [19].

3.4. Long-time asymptotic

The long-time asymptotics of the CH equation were obtained within the Riemann-Hilbert analysis context [13, 21]. Subject to a suitable initial condition satisfying (5) and (6), Boutet de Monvel et al. [13, 21] showed that the asymptotics of CH equation can be classified into different types in (x, t) domain. After a sufficiently long time, the regions can be divided into the (i) soliton region, (ii), (iii) two oscillatory regions, and (iv) fast decay region. Two transition regions denoted by (T1) exist between the regions (i) and (ii). The (T2) region between the regions (iii) and (iv) can be also seen in Fig. 2 and 3. We will confirm the existence of these regions by virtue of the space-time finite difference method detailed in Section 4. In (T1) and (T2) regions, the solutions to the CH equation asymptotically approach to the solutions of the Painlevé II transcendents

$$\frac{d^2w}{dz^2} = 2w^3 + zw \tag{21}$$

fixed by the asymptotics

$$w\left(z\right) \sim \rho \mathrm{Ai}\left(z\right) \text{ as } z \to \infty,\ z \in \mathbb{R}$$

where $\mathrm{Ai}(z)$ is the Airy function (see [13]).

The regions (ii) and (iii) result from the fact that the reflection coefficient $R(k)$ in scattering data is non-zero. On the other hand, if $R(k) \equiv 0$ (i.e., only discrete eigenvalues exist), oscillatory solutions are not observed. Under the circumstances, only the multi-soliton solutions are permitted to appear [11].

4. The solution in space-time domain

In this section, for the sake of clarity, we will briefly introduce the finite difference method employed to solve the CH equation in space-time domain. For the details of this method, one can refer to the paper [20].

Given an initial condition $u(x, 0) \in H^1$, where H^1 is the Sobolev space, the CH equation investigated at the critical shallow water speed, which is zero, has been shown to have the well-known conservation law $M = \int_{-\infty}^{\infty} u dx = \text{constant} := c_1$. The other conservation quantities are expressed as $\frac{1}{2}\int_{-\infty}^{\infty} u^2 + (u_x)^2 dx = \text{constant} := c_2$ (Hamiltonian H_1) and $\frac{1}{2}\int_{-\infty}^{\infty} u^3 + u(u_{xx})^2 dx$ constant $:= c_3$ (Hamiltonian H_2). The Hamiltonian $H_1 = \frac{1}{2}\int_{-\infty}^{\infty} u^2 + (u_x)^2 dx$ has association with the energy density $u^2 + (u_x)^2$.

4.1. Symplecticity and dispersion relation equation preserving finite difference scheme in space-time domain

Given a set of properly prescribed boundary condition and initial condition for $u(x, 0) \in H^1$, the space-time solution to (1) can be sought from the following equivalent inhomogeneous nonlinear hyperbolic pure advection equation for u to avoid approximating the mixed space-time derivative terms and the third-order dispersive term

$$u_t + uu_x = -P_x. \tag{22}$$

The above pressure-like term P is governed by the following elliptic Helmholtz equation

$$P - P_{xx} = u^2 + \frac{1}{2}u_x^2 + 2\kappa u. \tag{23}$$

4.2. Approximation of spatial derivatives

Within the framework of the combined compact difference (CCD) schemes, the derivative terms $\frac{\partial u}{\partial x}$ and $\frac{\partial^2 u}{\partial x^2}$ in (1.1) are approximated implicitly in a three-point grid stencil as follows for the case of $u > 0$

$$\begin{aligned} a_1 \frac{\partial u}{\partial x}|_{i-1} &+ \frac{\partial u}{\partial x}|_i + a_3 \frac{\partial u}{\partial x}|_{i+1} \\ &= \frac{1}{h}(c_1 u_{i-2} + c_2 u_{i-1} + c_3 u_i) \\ &\quad - h\left(b_1 \frac{\partial^2 u}{\partial x^2}|_{i-1} + b_2 \frac{\partial^2 u}{\partial x^2}|_i + b_3 \frac{\partial^2 u}{\partial x^2}|_{i+1}\right), \end{aligned} \tag{24}$$

$$\begin{aligned} -\frac{1}{8}\frac{\partial^2 u}{\partial x^2}|_{i-1} &+ \frac{\partial^2 u}{\partial x^2}|_i - \frac{1}{8}\frac{\partial^2 u}{\partial x^2}|_{i+1} \\ &= \frac{3}{h^2}(u_{i-1} - 2u_i + u_{i+1}) - \frac{9}{8h}\left(-\frac{\partial u}{\partial x}|_{i-1} + \frac{\partial u}{\partial x}|_{i+1}\right). \end{aligned} \tag{25}$$

The coefficients shown in (25), which can be determined partly from the modified equation analysis, by performing Taylor series expansion on the terms u_{i-1}, u_{i+1}, $\frac{\partial u}{\partial x}|_{i-1}$, $\frac{\partial u}{\partial x}|_i$, $\frac{\partial u}{\partial x}|_{i+1}$, $\frac{\partial^2 u}{\partial x^2}|_{i-1}$, $\frac{\partial^2 u}{\partial x^2}|_i$ and $\frac{\partial^2 u}{\partial x^2}|_{i+1}$ shown in (24) with respect to u_i to yield a formal accuracy order of six [27]. The other algebraic equation derived to uniquely determine all the introduced coefficients is based on the strategy of reducing dispersion error by matching the exact and numerical wavenumbers. For the details of maximizing dispersion accuracy, one can refer to [20, 28].

By virtue of these two rigorous analyses, $a_1 = 0.888251792581$, $a_3 = 0.049229651564$, $b_1 = 0.150072398996$, $b_2 = -0.250712794122$, $b_3 = -0.012416467490$, $c_1 = 0.016661718438$, $c_2 = -1.970804881023$ and $c_3 = 1.954143162584$ can be obtained. The resulting upwinding difference scheme

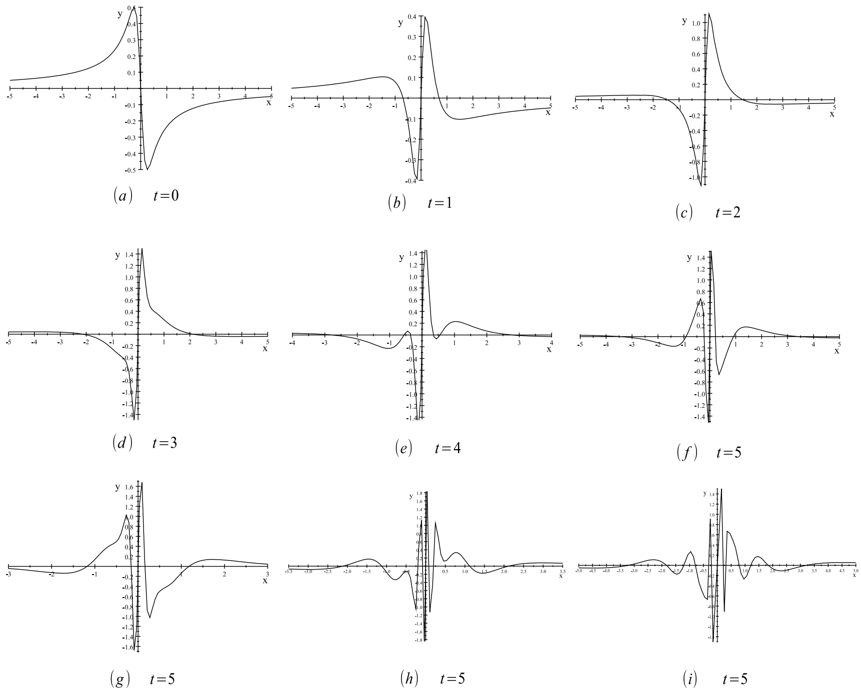

Figure 6: The time dependence of $\Im\big(R(k,t)\big)$ from $t=0$ to $t=15$ at $q_0=\frac{1}{2}$.

developed in a stencil of three grid points $i-1$, i and $i+1$ for $\frac{\partial u}{\partial x}$ has the spatial accuracy of order six according to the derived modified equation, namely, $\frac{\partial u}{\partial x} = \frac{\partial u}{\partial x}|_{\text{exact}} + 0.424003657 \times 10^{-6} h^6 \frac{\partial^7 u}{\partial x^7} + H.O.T.$ As $u<0$, the three-point non-centered CCD scheme can be similarly derived.

The three-point combined compact difference (CCD) scheme [29] is used here to approximate the gradient term P_x shown in (22) as follows

$$\begin{aligned} &\frac{h}{16}\frac{\partial^2 P}{\partial x^2}|_{i-1} - \frac{h}{16}\frac{\partial^2 P}{\partial x^2}|_{i+1} \\ &\quad = \frac{15}{16h}(-P_{i-1}+P_{i+1}) + \left(\frac{7}{16}\frac{\partial P}{\partial x}|_{i-1} + \frac{\partial P}{\partial x}|_i + \frac{7}{16}\frac{\partial P}{\partial x}|_{i+1}\right), \end{aligned} \tag{26}$$

$$\begin{aligned} &-\frac{1}{8}\frac{\partial^2 P}{\partial x^2}|_{i-1} + \frac{\partial^2 P}{\partial x^2}|_i - \frac{1}{8}\frac{\partial^2 P}{\partial x^2}|_{i+1} \\ &\quad = \frac{1}{h^2}(3P_{i-1} - 6P_i + 3P_{i+1}) - \frac{1}{h}\left(-\frac{9}{8}\frac{\partial P}{\partial x}|_{i-1} + \frac{9}{8}\frac{\partial P}{\partial x}|_{i+1}\right). \end{aligned} \tag{27}$$

The above centered CCD scheme developed in a grid stencil involving three

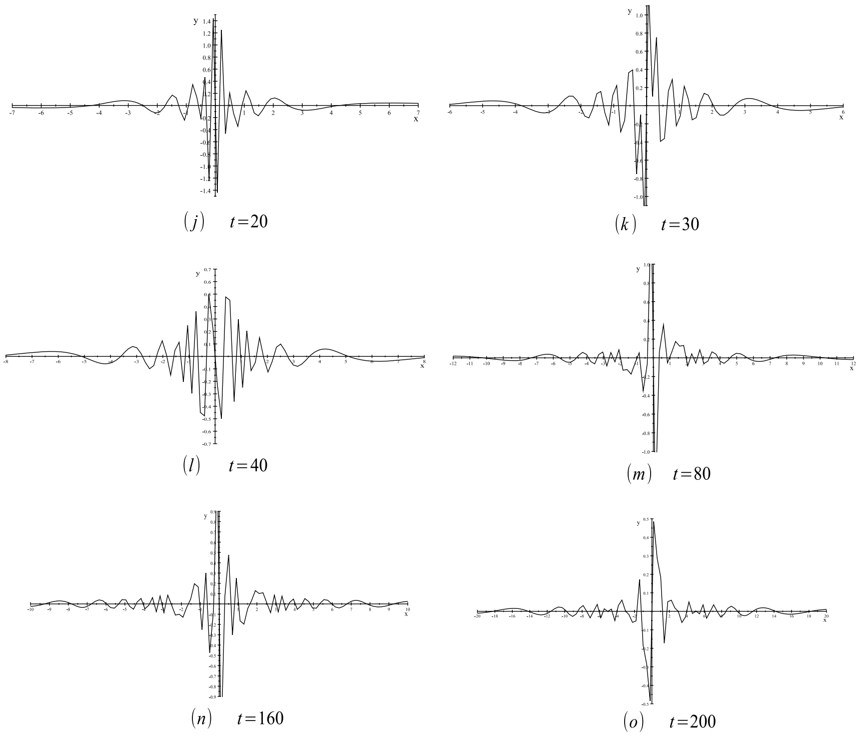

Figure 7: The time dependence of $\Im\big(R(k,t)\big)$ from $t = 20$ to $t = 200$ at $q_0 = \frac{1}{2}$.

points $i-1$, i and $i+1$ for $\frac{\partial P}{\partial x}$ yields the sixth-order accuracy.

The Helmholtz equation (or equation (23)) for P_i is approximated as follows for $g_i = -(u_i^2 + u_i u_{x,i})$

$$
\begin{aligned}
&P_{i+1} - \left(2 + h^2 + \frac{1}{12}h^4 + \frac{1}{360}h^6\right) P_i + P_{i-1} \\
&= h^2 g_i + \frac{1}{12}h^4 \left(f_i + \frac{\partial^2 g_i}{\partial x^2}\right) + \frac{1}{360}h^6 \left(g_i + \frac{\partial^2 g_i}{\partial x^2} + \frac{\partial^4 g_i}{\partial x^4}\right).
\end{aligned}
\tag{28}
$$

According to the corresponding modified equation for equation (23), which is $\frac{\partial^2 P}{\partial x^2} - P = g + \frac{h^6}{20160}\frac{\partial^8 P}{\partial x^8} + \frac{h^8}{1814400}\frac{\partial^{10} P}{\partial x^{10}} + \cdots + H.O.T.$, the proposed three-point compact differencing scheme is deemed sixth-order accurate.

4.3. Approximation of temporal derivatives

Due to the symplectic structure inherent in the CH equation, the time-stepping scheme for equation (22) cannot be chosen arbitrarily provided that one wishes to obtain a long-term accurate solution. To conserve this property in the currently investigated non- dissipative Hamiltonian system of equations (22-23), the following sixth-order accurate symplectic Runge-Kutta scheme [30] is applied to compute the CH solution iteratively for $u_t = F(u, P) = -uu_x - P_x$

$$u^{(1)} = u^n + \Delta t \left[\frac{5}{36}F^{(1)} + (\frac{2}{9} + \frac{2\tilde{c}}{3})F^{(2)} + (\frac{5}{36} + \frac{\tilde{c}}{3})F^{(3)} \right], \tag{29}$$

$$u^{(2)} = u^n + \Delta t \left[(\frac{5}{36} - \frac{5\tilde{c}}{12})F^{(1)} + (\frac{2}{9})F^{(2)} + (\frac{5}{36} + \frac{5\tilde{c}}{12})F^{(3)} \right], \tag{30}$$

$$u^{(3)} = u^n + \Delta t \left[(\frac{5}{36} - \frac{\tilde{c}}{3})F^{(1)} + (\frac{2}{9} - \frac{2\tilde{c}}{3})F^{(2)} + \frac{5}{36}F^{(3)} \right], \tag{31}$$

$$u^{n+1} = u^n + \Delta t \left[\frac{5}{18}F^{(1)} + \frac{4}{9}F^{(2)} + \frac{5}{18}F^{(3)} \right]. \tag{32}$$

In the above, $\tilde{c} = \frac{1}{2}\sqrt{\frac{3}{5}}$ and $F^{(i)} = F(u^{(i)}, P^{(i)})$, $i = 1, 2, 3$.

5. The solution in spectral domain

By means of the method of IST detailed in [6], the following scattering data can be rigorously derived [19, 20].

Theorem 5.1. *(Theorem 3.1 in [20]) Let $q_0 \in (0, 1)$ be a given constant and $A = \frac{q_0}{1-q_0}$. For the Camassa-Holm equation (1) subject to the initial condition (2), the scattering data can be derived as follows in spectral domain*

$$R\,(k) = \frac{-q_0}{q_0 + 2ik}, \;\; \mu_1 = \frac{q_0}{2}, \;\; \gamma_1 = \sqrt{\frac{q_0}{2}}. \tag{33}$$

In this section we will numerically solve the GLM equation under the initial condition (2).

5.1. Derivation on IST

The time dependent expressions of $R(k)$ and γ_j are derived in the following form [21]

$$R(k,t) = R(k)e^{-ikt/(1/4+k^2)}, \;\; \gamma_j\,(t) = \gamma_j e^{\mu_j t/2(1/4-\mu_j^2)}, \;\; \text{for } t > 0.$$

In (3.15), the expression of $f(z,t)$ can be written as

$$f(z,t) = \frac{q_0}{2} e^{\frac{2q_0}{1-q_0^2}t - \frac{q_0}{2}z} + \frac{1}{2\pi}\int_{-\infty}^{\infty} \frac{-q_0}{q_0+2ik} e^{i\left(kz - \frac{k}{1/4+k^2}t\right)} dk.$$

By the residue theorem, the integral term shown above can be simplified in a way similar to the KdV equation featuring with the initial condition of the delta function type [31, 32]. That is, $f(z,t)$ can be rewritten as

$$f(z,t) = \begin{cases} \frac{q_0}{2} e^{\frac{2q_0}{1-q_0^2}t - \frac{q_0}{2}z} & \text{for } z < 0, \\ \frac{q_0}{4} & \text{for } z = 0, \\ 0 & \text{for } z > 0. \end{cases} \tag{34}$$

In the first step of IST, the GLM equations (15) and (34) are solved by the underlying idea given in [33]. For simplicity, in the processes of performing IST the parameter t is omitted. The variable y is considered in the bounded interval $[-n, n]$. Provided that the domain $[-n, n]$ is partitioned into N parts, the grid size turns out to be $h = \frac{2n}{N}$. Then, the discrete variables y_i, r_j, z_m are defined as

$$\begin{aligned} y_i &= -n + (i-1)h,\ i = 1, ..., N+1, \\ r_j &= -n + (j-1)h,\ j = 1, ..., N+1, \\ z_m &= -n + (m-1)h,\ m = 1, ..., N+1. \end{aligned}$$

Let $K(y_i, r_j) = K_{ij}$, and $f(y_i + r_j) = f_{ij}$, equation (15) can then be approximated using the trapezoidal integration rule

$$K_{ij} + f_{ij} + h\sum_{m=i}^{N+1} \Delta_{im} K_{im} f_{jm} = 0, \quad i \le j \le N+1 \tag{35}$$

where

$$\Delta_{ik} = \begin{cases} \frac{1}{2} & \text{for } k = i,\ N+1, \\ 1 & \text{otherwise.} \end{cases}$$

Our objective of solving (35) is to find $q(y_i, t)$. From (17), the discrete form of $q(y_i, t)$ is expressed as

$$q_i = q(y_i, t) = -2\left(\frac{K_{i+1,i+1} - K_{i,i}}{h}\right),\ i = 1, ..., N. \tag{36}$$

The forward difference scheme is chosen from the physical viewpoint. That is, the incident waves expressed in (12) move from right ($y \to \infty$) to left ($y \to -\infty$), Like the application of the upwinding schemes in solving the hyperbolic PDEs, the potential $q(y)$ at $y = y_i$ shall be influenced by q at $y = y_{i+1}$.

Following similar process given in [33], equation (35) is simplified as follows. For $i = N+1$, we have $j = N+1$. Then, (35) is considered as a degenerate case. In this case we set $K_{N+1,N+1} = -f_{N+1,N+1} = 0$. For $i \le N$, let $F_i = \text{prin}_{i+1}(F)$ be the principal sub-matrix of order $i+1$, where

$$F := \begin{pmatrix} f_{N+1,N+1} & \cdots & f_{N+1,1} \\ \vdots & \ddots & \vdots \\ f_{1,N+1} & \cdots & f_{1,1} \end{pmatrix},$$

and f_i^T be the last row of F_i. Similarly, let $K_i = \text{prin}_{i+1}(K)$, where

$$K = \begin{pmatrix} K_{N+1,N+1} & \cdots & K_{N+1,1} \\ \vdots & \ddots & \vdots \\ K_{1,N+1} & \cdots & K_{1,1} \end{pmatrix},$$

and k_i^T be the last row of K_i. By writing $S_i = \text{diag}(\Delta_{N+1-i,N+1}, \ldots, \Delta_{N+1-i,N+1-i})$, equation (35) can be expressed differently as

$$(I_{i+1} + hF_iS_i)\, k_i = -f_i.$$

It should be noticed that $I_{i+1} + hF_iS_i$ is not a positive definite matrix. Unlike the work carried out in [33], we need to compute k_i in a direct way. Let $K_{N+2,N+2}$ be the polynomial extrapolation

$$K_{N+2,N+2} = \frac{1}{h + 2n - 2Nh}(4(n - Nh)K_{N+1,N+1} + (h - 2n + 2Nh)K_{N,N}).$$

To compute $q_{N+1,}$ the forward difference scheme is applied.

The next derivation step is to recover the momentum variable $w(y)$ from $q(y)$. This step is the most difficult part in IST analysis. More importantly, this step clearly shows the primary difference between the IST analysis of the CH and KdV equations in the sense that the recovery from $q(y)$ to $w(y)$ needs to proceed a nonlinear process rather than its linear counterpart for the KdV equation.

We can find the solution $\psi(y)$ of $\phi_{yy} = \left(q(y) + \frac{1}{4}\right)\phi$ with the asymptotics (19) by solving the following integral equation.

$$\psi(y) = e^{-\frac{y}{2}} + \int_y^\infty \left(e^{\frac{\xi-y}{2}} - e^{\frac{y-\xi}{2}}\right) q(\xi)\,\psi(\xi)\,d\xi,\ \ y \in \mathbb{R}.$$

The discrete version for the above integral equation is expressed as

$$\psi(y_i) := \psi_i = e_i + h\sum_{k=i}^{N+1} \Delta^f_{i,k} E_{ik} q(\xi_k)\,\psi(\xi_k),$$

where $E_{ik} = e^{\frac{\xi_k - y_i}{2}} - e^{\frac{y_i-\xi_k}{2}}$, $\xi_k = -n + (k-1)h$, $e_i = e^{-\frac{y_i}{2}}$,

$$\Delta^f_{ik} = \begin{cases} \frac{1}{2} & \text{for } k = i,\ k = N+1, \\ 1 & \text{otherwise.} \end{cases}$$

Finally, we can obtain the equation

$$\left(I_{N+1} - hE^0 \mathrm{diag}(q_i)\right)\Psi = \mathbf{e}$$

where

$$\Psi = \begin{pmatrix} \psi_1 \\ \psi_2 \\ \vdots \\ \vdots \\ \psi_{N+1} \end{pmatrix}, \quad \mathbf{e} = \begin{pmatrix} e_1 \\ \vdots \\ \vdots \\ \vdots \\ e_{N+1} \end{pmatrix},$$

$$E^0 = \begin{pmatrix} 0 & E_{12} & \cdots & E_{1N} & \frac{E_{1,N+1}}{2} \\ 0 & 0 & \ddots & \vdots & \vdots \\ & \ddots & \ddots & E_{N-1,N} & \vdots \\ & \ddots & \ddots & 0 & \frac{E_{N,N+1}}{2} \\ 0 & & 0 & 0 & 0 \end{pmatrix}.$$

The next step is to find $\psi^4\left(H_t^{-1}(e^x), t\right)$ through (20). Recall that $H_t(y) = \int_{-\infty}^y \frac{1}{\psi^2(\xi,t)}d\xi = e^x$. From the values of $\Psi = (\psi_1, ..., \psi_{N+1})^T$, the discrete representation of $H_t(y)$ can be expressed as

$$H_i := H(y_i) = h\sum_{k=1}^{i} \Delta_{i,k}^{H} \frac{1}{\psi^2(\xi_k)} \tag{37}$$

where

$$\Delta_{ik}^{H} = \begin{cases} \frac{1}{2} & \text{for } k=1,\ k=i, \\ 1 & \text{otherwise.} \end{cases}$$

For $i=1$, we set $H_1=0$. Then, equation (37) is solved for $i=2,...,N+1$, thereby leading to

$$\begin{pmatrix} H_2 \\ \vdots \\ \vdots \\ H_{N+1} \end{pmatrix} = h \begin{pmatrix} \Delta_{2,1}^{H} & \Delta_{2,2}^{H} & \cdots & 0 \\ \vdots & \vdots & \ddots & \vdots \\ \Delta_{N+1,1}^{H} & \Delta_{N+1,2}^{H} & \cdots & \Delta_{N+1,N+1}^{H} \end{pmatrix} \begin{pmatrix} \frac{1}{\psi_1^2} \\ \vdots \\ \vdots \\ \frac{1}{\psi_{N+1}^2} \end{pmatrix}.$$

If one uses the resulting H_i as the data to perform IST analysis, the dependence of x on y cannot be accurately obtained and we need to add an error term to H_i. For $t=0$, we have $\int_{-\infty}^{-n} \frac{1}{\psi^2(\xi,0)} d\xi = \frac{4}{1+e^n}$ and use this as the error for all $t>0$. $\hat{H}_1,...,\hat{H}_{N+1}$ are therefore defined as $\hat{H}_i = H_i + \frac{4}{1+e^n}$.

The value of $H^{-1}(e^{x_i})$ can then be computed through interpolation for $(H_1,...,H_{N+1})$. When representing $w(x_i) = e^{2x_i}\psi^4\left(H^{-1}(e^{x_i})\right)$ in terms of x, we need to perform interpolation to find $w(x_i)$. In order to avoid generating unnecessary error, the momentum w and the solution u are expressed in terms of y. That is, we use the parametric expression $(w(y,t), x(y,t))$ (resp. $(u(y,t), x(y,t))$) to express $w(x,t)$ (resp. $u(x,t)$) with y being considered as a parameter. By substituting $x(y_i) = \log H(y_i)$ into the momentum variable, we have

$$\begin{aligned} w_i := w(y_i) &= e^{2x(y_i)}\psi^4(y_i) \\ &= H^2(y_i)\,\psi^4(y_i), \end{aligned} \quad i=1,...,N+1. \tag{38}$$

The final step in the IST analysis is to recover u from w. Since we want to express u in y domain, we recast the equation $u-u_{xx}=w-1$ in x domain to the corresponding equation defined in y domain:

$$wu_{yy} + \frac{1}{2}w_y u_y - u = 1 - w$$

In the above equation, $\frac{dy}{dx} = \sqrt{w\left(y,t\right)}$. By performing a centered finite difference approximation on the above equation, we have

$$\begin{aligned}&\left(w_i + \frac{1}{8}\left(w_{i+1} - w_{i-1}\right)\right)u_{i+1} - \left(2w_i + h^2\right)u_i + \left(w_i - \frac{1}{8}\left(w_{i+1} - w_{i-1}\right)\right)u_{i-1}\\ &\quad = -h^2\left(w_i - 1\right),\ i = 2, ..., N.\end{aligned}$$

or

$$\begin{aligned}A\begin{pmatrix} u_N \\ u_{N-1} \\ \vdots \\ u_3 \\ u_2 \end{pmatrix} &= \left(-h^2\right)\begin{pmatrix} w_N - 1 \\ w_{N-1} - 1 \\ \vdots \\ w_3 - 1 \\ w_2 - 1 \end{pmatrix}\\ &+\begin{pmatrix} -\left(w_N + \frac{1}{8}\left(w_{N+1} - w_{N-1}\right)\right)u_{N+1} \\ 0 \\ \vdots \\ 0 \\ -\left(w_2 - \frac{1}{8}\left(w_3 - w_1\right)\right)u_1 \end{pmatrix}\end{aligned} \tag{39}$$

The components of the above matrix $A = \left(A_{ij}\right)_{1\leq i,j\leq N-1}$ are defined as

$$\begin{aligned}&A_{ii} = -\left(2w_{N+1-i} + h^2\right), \text{for } i = 1, ..., N-1,\\ &A_{i,i+1} = w_{N+1-i} - \frac{1}{8} * \left(w_{N+2-i} - w_{N-i}\right), \text{for } i = 1, ..., N-2,\\ &A_{i,i-1} = w_{N+1-i} + \frac{1}{8} * \left(w_{N+2-i} - w_{N-i}\right), \text{for } i = 2, ..., N-1,\\ &A_{i,j} = 0,\ \text{otherwise},\end{aligned}$$

Note that u_1 and u_{N+1} are interpolated by the Lagrange polynomial formula, thereby yielding

$$\begin{aligned}u_1 &= u_2\frac{\left(y_1 - y_3\right)\left(y_1 - y_4\right)}{\left(y_2 - y_3\right)\left(y_2 - y_4\right)} + u_3\frac{\left(y_1 - y_2\right)\left(y_1 - y_4\right)}{\left(y_3 - y_2\right)\left(y_3 - y_4\right)} + u_4\frac{\left(y_1 - y_2\right)\left(y_1 - y_3\right)}{\left(y_4 - y_2\right)\left(y_4 - y_3\right)}\\ &= 3u_2 - 3u_3 + u_4;\end{aligned}$$

$$u_{N+1} = u_N\frac{\left(y_{N+1} - y_{N-1}\right)\left(y_{N+1} - y_{N-2}\right)}{\left(y_N - y_{N-1}\right)\left(y_N - y_{N-2}\right)}$$

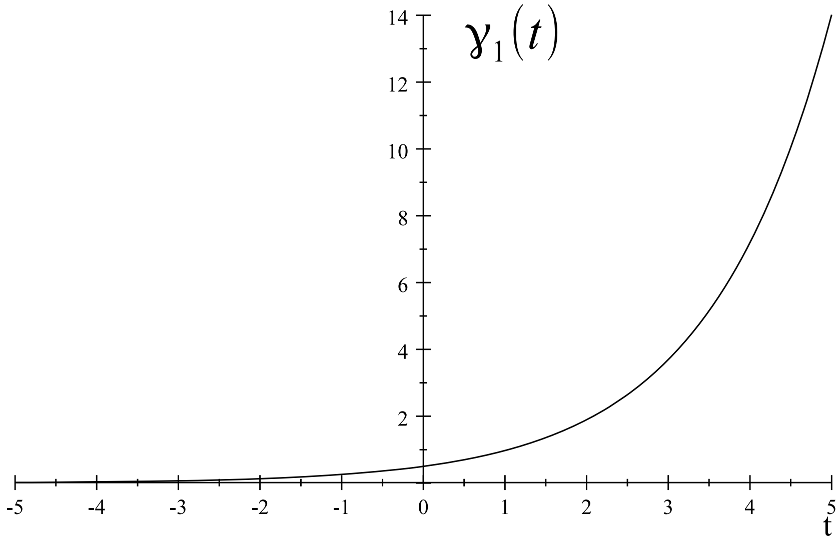

Figure 8: The graph of $\gamma_1(t)$ is plotted with respect to t at $q_0 = \frac{1}{2}$.

$$
\begin{aligned}
&+ u_{N-1}\frac{(y_{N+1}-y_N)(y_{N+1}-y_{N-2})}{(y_{N-1}-y_N)(y_{N-1}-y_{N-2})} \\
&+ u_{N-2}\frac{(y_{N+1}-y_N)(y_{N+1}-y_{N-1})}{(y_{N-2}-y_N)(y_{N-2}-y_{N-1})} \\
&= 3u_N - 3u_{N-1} + u_{N-2}.
\end{aligned}
$$

6. Numerical study of the influence of transmition/reflection coefficients on the solutions

Under the initial condition (2), we recall that the time evolution of the reflection and normalization coefficients are expressed respectively as $R(k,t) = R(k)e^{-ikt/(1/4+k^2)} = \frac{-q_0}{q_0+2ik}e^{-ikt/(1/4+k^2)}$ and $T(k,t) = T(k) = \tilde{T}(k)\,e^{ikH_{-1}(w)}$. For the derivation of the scattering data and $H_{-1}(w)$, one can refer to [19].

In order to explain the influence of the reflection coefficient $R(k,t)$ on the computed solutions $u(y,t)$ at different times, we plot the profiles of $R(k,t)$ in Fig. 4 and Fig. 5. From the above derived expression for $R(k,t)$, we know that $R(0,t) = -1$ for all $t \geq 0$. In Figs. 4 and 5, the height of $\Re\big(R(k,t)\big)$ is increased with respect to time t. Moreover, Figs. 6 and 7 reveal that $\Im\big(R(k,t)\big)$ changes its profile shape, from the maximum appearing in the left to that appearing in the right. All the four figures show that the heights of $\Re\big(R(k,t)\big)$ and the amplitudes of $\Im\big(R(k,t)\big)$ change more abruptly as time increases. According to the definition of reflection coefficient, at a larger time the profile of $\gamma_1(t) = \gamma_1 e^{\frac{\mu_1 t}{2(1/4-\mu_1^2)}} = \sqrt{\frac{q_0}{2}} e^{\frac{q_0}{1-q_0^2}t}, \forall t > 0$ is also plotted in Fig. 8.

7. Concluding remarks

In this article, we continue our work in [20] on the long-time asymptotics of the Camassa-Holm equation. In the works of Boutet de Monvel [13, 21], there exist some asymptotic solution formulas. However, what the solution profiles look like and how the space-time domain information corresponding to the solution in spectral domain are not clear. In the so-called "spectral domain", the solutions are not solved in the original space-time domain but rather we intend to apply the inverse scattering transform (IST) method underlying the characteristics of integrable system. The Gelfand-Levitan-Marchenko (GLM) integral equations are discretized first to get the potential $q(y,t)$ of the transformed Schrödinger type operator. Then, in the inverse process of the CH equation, which is different from that of the KdV equation, we transform the equation from the potential $q(y,t)$ to the momentum $w(y,t)$ and then perform the change of variables from y to x from their relation (8). However, due to the computational difficulty encountered in the numerical integration of GLM, which involves the term e^t in the example of the one-soliton solution of KdV equation, the current computational accuracy is insufficient for the case at a large time. Therefore, it is difficult at the time being to predict a very accurate solution at a large time. Our IST results can however give us a conceptual guidance of making a comparison of results using the finite difference and the IST methods at an early time of the wave propagation.

Acknowledgments

The corresponding author, professor Tony Wen-Hann Sheu, would like to thank professor Chang-Shou Lin for his encouragement and support of performing this study.

References

[1] R. Camassa and D. D. Holm, *An integrable shallow water equation with peaked solitons*, Phys. Rev. Lett., 71 (1993), pp. 1661–1664. MR1234453

[2] B. Fuchssteiner and A. Fokas, *Symplectic structures, their Bäcklund transformation and hereditary symmetries*, Phys. D, 4 (1981/82), pp. 47–66. MR0636470

[3] A. Constantin and D. Lannes, *The hydrodynamical relevance of the Camassa-Holm and Degasperis-Procesi equations*, Arch. Ration. Mech. Anal., 192 (2009), pp. 165–186. MR2481064

[4] D. Ionescu-Kruse, *Variational derivation of the Camassa-Holm shallow water equation*, J. Nonlinear Math. Phys., 14 (2007), pp. 303–312. MR2350091

[5] R. S. Johnson, *Camassa-Holm, Korteweg-de Vries and related models for water waves*, J. Fluid Mech., 455 (2002), pp. 63–82. MR1894796

[6] A. Constantin, *On the scattering problem for the Camassa-Holm equation*, R. Soc. Lond. Proc. Ser. A Math. Phys. Eng. Sci., 457 (2001), pp. 953–970. MR1875310

[7] A. Constantin, *Existence of permanent and breaking waves for a shallow water equation: a geometric approach*, Ann. Inst. Fourier (Grenoble), 50 (2000), pp. 321–362. MR1775353

[8] P.H. Chiu, L. Lee, T.W.H. Sheu, *A dispersion–relation-preserving algorithm for a nonlinear shallow-water wave equation*, J. Comput. Phys., 228 (2009), pp. 8034–8052. MR2573344

[9] P.H. Chiu, L. Lee and T.W.H. Sheu, *A sixth-order dual preserving algorithm for the Camassa–Holm equation*, J. Comput. Appl. Math., 233 (2010), pp. 2267–2278. MR2592253

[10] T. W. H. Sheu, P. H. Chiu and C. H. Yu, *On the development of a high-order compact scheme for exhibiting the switching and dissipative solution natures in the Camassa-Holm equation*, J. Comput. Phys. 230 (2011), 5399–5416. MR2799516

[11] R. S. Johnson, *On solutions of the Camassa-Holm equation*, R. Soc. Lond. Proc. Ser. A Math. Phys. Eng. Sci., 459 (2003), pp. 1687–1708. MR1997519

[12] N. J. Zabusky and M. D. Kruskal, *Interaction of solutions in a collisionless plasma and the recurrence of initial states*, Phys. Rev. Letters, 15 (1965), pp. 240–243.

[13] A. Boutet de Monvel, A. Its and D. Shepelsky, *Painlevé-type asymptotics for the Camassa-Holm equation*, SIAM J. Math. Anal., 42 (2010), pp. 1854–1873. MR2679598

[14] A. Constantin and J. Lenells, *On the inverse scattering approach to the Camassa–Holm equation*, J. Nonlinear Math. Phys. 10 (2003), pp.252–255. MR1990677

[15] C. S. Gardner, J. M. Greene, M. D. Kruskal and R. M. Miura, *Korteweg-de Vries equation and generalizations. VI. Methods for exact solution*, Comm. Pure Appl. Math., 27 (1974), pp. 97–133. MR0336122

[16] M. J. Ablowitz, D. J. Kaup, A. C. Newell and H. Segur, *The inverse scattering transform-Fourier analysis for nonlinear problems*, Studies in Appl. Math., 53 (1974), pp. 249–315. MR0450815

[17] G. Teschl, *Inverse scattering transform for the toda hierarchy*. Math. Nach. 202 (1999), pp. 163–171. MR1694723

[18] M.V. Wickerhauser, *Inverse scattering for the heat operator and evolutions in 2+1 variables*, Comm. Math. Phys., 108 (1987), pp. 67–89. MR0872141

[19] C. H. Chang and Tony W. H. Sheu, *On a spectral analysis of scattering data for the Camassa-Holm equation*, J. Nonlinear Math. Phys., 22, No. 1 (2015), pp. 102–116. MR3286736

[20] C. H. Chang, C. H. Yu and Tony W. H. Sheu, *Long-time asymptotic solution structure of Camassa-Holm equation subject to an initial condition with non-zero reflection coefficient of the scattering data*, J. Mathematical Physics, 57 (2016), 103508. MR3565958

[21] A. Boutet de Monvel, A. Kostenko, D. Shepelsky and G. Teschl, *Long-time asymptotics for the Camassa-Holm equation*, SIAM J. Math. Anal., 41 (2009), pp. 1559–1588. MR2556575

[22] P. Deift and E. Trubowitz, *Inverse scattering on the line*, Comm. Pure Appl. Math., 32 (1979), pp. 121–251. MR0512420

[23] A. Constantin and R. Ivanov, *Poisson structure and action-angle variables for the Camassa-Holm equation*, Lett. Math. Phys., 76 (2006), pp. 93–108. MR2223766

[24] A. Constantin, J. Lenells, *On the inverse scattering approach for an integrable shallow water wave equation*, Phys. Lett. A 308 (2003), pp. 432–436. MR1977363

[25] T. J. Bridges and S. Reich, *Multi-symplectic integrators: numerical schemes for Hamiltonian PDEs that conserve symplecticity*, Phys. Lett. A, 284 (2001), pp. 184–193. MR1854689

[26] D. Cohen, B. Owren and X. Raynaud, Multi-symplectic integration of the Camassa–Holm equation, J. Comput. Phys. 227 (2008), pp. 5492–5512. MR2414917

[27] P. C. Chu and C. Fan, *A three-point combined compact difference scheme*, J. Comput. Phys., 140 (1998), pp. 370–399. MR1616146

[28] C. K. W. Tam and J. C. Webb, *Dispersion-relation-preserving finite difference schemes for computational acoustics*, J. Comput. Phys., 107 (1993), pp. 262–281. MR1229226

[29] G. Ashcroft and X. Zhang, *Optimized prefactored compact schemes*, J. Comput. Phys., 190 (2003), pp. 459 – 477.

[30] W. Oevel and M. Sofroniou, *Symplectic Runge-Kutta Schemes II: Classification of symmetric methods*, University of Paderborn, Germany, 1997. MR1472210

[31] P. G. Drazin and R. S. Johnson, *Solitons: an Introduction*, Cambridge Texts in Applied Mathematics, Cambridge University Press, Cambridge, 1989. MR0985322

[32] G. B. Whitham, *Linear and Nonlinear Waves*, Wiley-Interscience [John Wiley & Sons], New York-London-Sydney, 1974. Pure and Applied Mathematics. MR0483954

[33] O. Hald, *Numerical solution of the Gel'Fand-Levitan equation*, Linear Algebra Appl., 28 (1979), pp. 99–111. MR0549424

Chueh-Hsin Chang
Department of Applied Mathematics
Tunghai University
Taichung
Taiwan
E-mail address: changjuexin@thu.edu.tw

Ching-Hao Yu
State key lab of Hydraulics and Mountain River Engineering
Sichuan University
Sichuan 610000
P.R. China
E-mail address: Chyu@zju.edu.cn

Tony Wen-Hann Sheu
Department of Engineering Science and Ocean Engineering
National Taiwan University
Taipei
Taiwan
E-mail address: twhsheu@ntu.edu.tw

Received May 10, 2019